Circular Dichroism and Fluorescence Spectroscopic Study of RNA-protein Folding Patterns in Human hnRNP A3 and Their Implications in Human Autoimmune Diseases

E. SÜLEYMANOĞLU[1,2] *

([1] *Institute of Biochemistry, University of Vienna, Medical Faculty, Vienna Biocenter, Dr. Bohr-Gasse 9/3, A-1030, Vienna, Austria;* [2] *Institute Curie, Centre Unversité Paris-Sud, Bât. 110, Genetics and Chemistry of Eukaryotic Genomes, Laboratory of Mutagenesis and Carcinogenesis, 91405 Orsay, France*)

Abstract In human cells, the heterogeneous nuclear ribonucleoproteins (hnRNP) are represented by a group of polypeptides, with various molecular properties, comprizing the most abundant constituents of the cell nucleus. Autoantibodies to hnRNPs have been reported in patients suffering from different rheumatic dieseases since 1980s. Experimental evidence indicates that hnRNP complexes undergo substantial structural changes during mRNA formation and export. However, how this contributes to disease development still has to be elucidated. Here some preliminary physicochemical features of RNA-protein folding and stability patterns of newly characterized hnRNP A3 with further functional implications in development of systemic human autoimmune states are reported.

Key words autoimmunity, hnRNP proteins, RNA-protein interactions, circular dichroism, fluorescence spectroscopy

The A/B type heterogeneous nuclear ribonucleoproteins (hnRNP A/B) form a subgroup of closely related proteins which are characterized by a common general structure: their N-terminal part consist of two adjacent RNA binding domains (RBD), whereas the C-terminal part contains a glycine-rich auxiliary domain. In humans three members of the hnRNP A/B family have been identified so far: A0, A1/A1^{B} and A2/B1. We have described recently the new member of hnRNP A/B group with yet undescribed funtions[1]. It is now well-established that hnRNP particles play a role as autoantigens and that they are targeted by patients' autoantibodies in a more or less disease-specific manner[2,3]. Interestingly, the major epitope is typically recognized differently by antibodies from patients suffering from a variety of diseases, indicating the existance of disease-specific recognition patterns of hnRNP autoantigens which might be useful for differential diagnosis of rheumatic autoimmune diseases[4]. A characteristic feature seen in many human rheumatic diseases is the presence of antinuclear antibodies, their targets being the nucleic acid-protein complexes in the nucleus, such as DNA-protein complexes and ribonucleoproteins. Autoantibodies to DNA-protein complexes can be directed against double-stranded DNA (dsDNA), and chromatin compounds, particularly against histones, as well as against various proteins engaged in nucleic acid metabolism, such as DNA topoisomerase-Ⅰ, proliferating cell nuclear antigen (PCNA), Ku and centromere proteins. On the other hand, autoantibodies synthesized against ribonucleoprotein complexes are usually directed to their protein components, such as ribosomal proteins, U snRNP proteins and tRNA synthetases, although occasionally the RNAs may also be targeted, as demonstrated for 28 S rRNA, U1 snRNA or tRNA[2~4]. snRNPs and hnRNPs are considered to be the major components of the spliceosome, interacting closely during mRNA processing. Since many subcellular autoantigens are parts of greater biomacromolecular assemblages, such as the nucleolus, or the ribosome, it is easy to appreciate why the spliceosome, or certain parts of it are autoimmune targets. This complex would then create different autoimmune responses in different groups of patients with related diseases. Majority of studies on these macromolecular assemblies are at the cDNA level with subsequent study of immunochemical properties of their tissue-specific gene expression patterns. Our efforts concentrate on certain underestimated biophysical issues with particular emphasis on their functional implications and relevance to development of disease-specific epitope formation. RNA-protein binding modes were studied in other hnRNP A/B proteins, mainly in terms of molecular biology of pre-mRNA processing. Their possible role in autoepitope formation was not approached and thus the significance of these findings in this context remains obscure. Some experimental evidence concerning the possible implications of RNA-protein folding patterns of our newly characterized human hnRNP A3[1] protein are outlined here as a model, for comparative reasons. Some preliminary results of this approach were also recently presented[5].

* Present address: Gazi Mahallesi, Polatlı Caddesi, No: 115/5, Yenimahalle, 06560-Ankara.
Tel: 00-90-312-211-19-47, Fax: 00-90-312-417-09-16
E-mail: sofia1967@bulgaria.com, sofia1967@abv.bg
Received: September 03, 2003 Accepted: October 31, 2003

1 Materials and methods

1.1 Sera from patients and controls

A total of 314 sera from patients with rheumatoid arthritis(RA), systemic lupus erythematosus(SLE), mixed connective tissue diesease (MCTD), scleroderma, CREST syndrome, polymyositis/dermatomyositis (PM/DM), Sjorgen's syndrome, reactive arthritis, psoriatic arthritis, osteoarthritis, respectively were used. Sera from healthy persons were used as negative controls.

1.2 Cloning, expression, isolation and immunochemical characterization of hnRNP A3

Recombinant hnRNP A3 was expressed in *E. coli* LysS strain, employing ligation independent cloning (LIC) system for cloning of PCR products. PCR (BiometraR, TRIO-Thermoblock PCR cycler) was used for cloning the cDNA of human hnRNP A3. To isolate the cDNA, human liver and brain cDNA libraries were screened by PCR using primers complementary to sequences in the 5′- and 3′-untranslated regions of the fetal brain (FBRNP) cDNA. cDNAs encoding fragments of hnRNP A3 were generated by PCR as deletion mutants.

1.3 DNA sequencing

All the DNA sequencing was performed by the Vienna Biocenter oligo team (http://emb1.bcc.univie.ac.at/gem). Nucleotide and deduced protein sequences of *Xenopus laevis* hnRNP A3, FBRNP, and human hnRNP A3 were aligned employing CLUSTALW programme (http://www2.ebi.ac.uk/clustalw/).

1.4 Affinity chromatography

Bacterially expressed hnRNP A3 and its parts were purified after initial optimization of purification conditions of the expressed fragment. 4 ml of the protein extract were spun down in 2 ml Eppendorf tubes of 14 000 r/min at 4℃. This step was repeated twice. The supernatant was filtered through 0.20 μm sterile filters (Millipore®) with a syringe. Afterwards, small-size Ni-NTA spin columns (QUIAGEN) were used. The columns were always stored at 4℃. Then, each column was treated with 600 μl of washing buffer (8 mol/L urea, 0.1 mol/L NaH_2PO_4, 0.01 mol/L Tris-HCl, pH = 6.3). Afterwards, the columns were spun down for 2 min at 4℃, at 2 000 r/min. The flowthrough was discarded. 600 μl of protein extract was applied per single column 4 times. The flowthrough was discarded and the columns were washed with washing buffer twice. Finally, each particular column was treated with 20 μl of elution buffer (8 mol/L urea, 0.1 mol/L NaH_2PO_4, 0.01 mol/L Tris-HCl, pH = 4.5) twice. The purified protein fragments were analysed by gel electrophoresis on 12% SDS polyacrylamide gels. Having optimized the protein purification conditions, the same procedure was carried out in a large-scale experimental setup. For this purpose, 10 ml of Ni-NTA agarose (QUIAGEN) was spun down at 3 000 r/min in FALCON® tube in Minifuge RF (Heraeus Sepatech) for 15 min at 4℃. This step was repeated twice. Afterwards, the supernatant was applied to a Column PD-10 (Pharmacia Biotech AB, Uppsala, Sweden). Alternatively, the Ni-NTA agarose was applied to original tube of BIO-RAD ECONO SYSTEM chromatography equipment (Bio-Rad Laboratories, 2000 Alfred Nobel Drive, Hercules, CA 94547, USA). In both cases, first the column was washed extensively until the UV-absorbance signal was minimal, or in the case of Column-PD-10, the washing step was repeated up to 6 times. 10 ~ 15 ml of protein extract was applied. The eluted protein fragments were collected in separate Eppendorf tubes and each of them was analysed by SDS-PAGE.

1.5 Epitope mapping

To characterize the major antibody-binding sites, various deletion mutants were created by PCR and bacterially expressed as His-tagged fusion proteins, as outlined above. The immune reactivity of the various fragments was investigated by immunoblotting using 12 selected hnRNP A3 positive sera, as described[1].

1.5.1 Circular dichroism spectroscopy: To avoid possible masking of protein spectra, additives and other stabilizimg compounds were avoided during all circular dichroism (CD) experiments. Throughout all the CD measurements, 0.5 g/L protein and 1 g/L RNA concentration in 5 mmol/L phosphate buffer, for maintaining protein stability were used. Cell- path length was variable, depending on the experimental conditions. For CD spectroscopy, full-length hnRNP A3 protein was purified as described above and dissolved in 8 mol/L urea. Renaturation was achieved by dialyzing extensively against 5 mmol/L phosphate buffer (pH = 7.2), using Spectraphor 2 dialysis membrane. CD spectra were measured using Jasco-J600 spectropolarimeter (Jasco Corp., Japan). Spectra were measured from 250 to 200 nm. To study renaturation of hnRNP A3, serial dilutions of the 8 mol/L urea were carried out in 5 mmol/L phosphate buffer (pH = 8.4). The elipticity of the individual samples at 220 nm was time-averaged for 200 time points, then duplicate experiments were averaged together. Afterwards baseline subtraction fitting of the measured CD data was done. Hysteresis experiments were performed as well following urea and temperature denaturation experiments.

1.5.2 Fluorescence spectroscopy: Steady-state fluorescence measurements were done to determine the forces stabilizing the RNP complex in general, or whether aromatic amino acids are involved in protein-nucleic acid binding, in particular. The affinitively

purified ribonucleoprotein fragments were dissolved in 1 ~ 1.5 ml phosphate buffer. The optimal fluorescence emission wavelength was searched for at 280 nm and the fluorescence was measured (Shimadzu fluorescence spectrometer). Having measured the absolute value of the RNP complexes' fluorescence, the salt dissociation was employed. Thus, the protein-nucleic acids complex was dissociated by adding NaCl and the flourescence of the dissociated complex was measured.

1.5.3 RNA-protein crosslink assay: 100 ng (0.3 μmol/L) of [^{32}P]-labelled oligoribonucleotide r(UUAGGG)$_4$ and 3 μmol/L purified recombinant hnRNP A3 or deletion mutants respectively were mixed and incubated at room temperature for 20 min in 20 μl of binding buffer (10 mmol/L Tris-HCl, pH 7.5, 1 mmol/L EDTA, 4% glycerol, 0.1% Triton-X 100, 10 mmol/L β-mercaptoethanol). The reaction mixtures were then transfered to a microtiter plate, put on ice and irradiated with an UV-lamp ("Stratalinker", Stratagene, USA) at 254 nm at a dose of 9.9 mJ/mm^2. After addition of Laemli sample buffer (50 mmol/L Tris-HCl, pH 6.8, 2% (*w/v*) SDS, 10% (*v/v*) glycerol, 5% (*w/v*) β-mercaptoethanol, 0.01% bromophenol blue), the samples were boiled for 10 min and analysed on 10% SDS-polyacrylamide gels. The gels were then dried and autoradiographed.

2 Results

2.1 Molecular characterization of hnRNP A3

Several human cDNA libraries were screened by PCR for the presence of hnRNP A3 cDNA. As a result, a cDNA was isolated from a human liver library encoding a protein of 296 amino acid residues, which showed a high homology, but was not identical to the fetal brain cDNA, as well as to both hnRNP A1 and A2. However, the highest degree of similarity was found with a cDNA, encoding a protein called *X*-hnRNP A3 from *Xenopus laevis*. Therefore, it is assumed that the human cDNA encodes human hnRNP A3. Expression of the liver cDNA in *E. coli* resulted in a 32 ku protein, whose autoreactivity was investigated by Western blotting, employing more than 300 sera from patients with rheumatic diseases. Autoantibodies were detected in 13/104 rheumatoid arthritis (RA) sera, in 7/56 systemic lupus erythemathosus (SLE) sera, 5/20 mixed connective tissue disease (MCTD) sera and 2/20 scleroderma patients' sera. Detailed epitope mapping studies reveal that hnRNP A3 presumably possesses two unique major epitopes, suggesting the existence of complicated conformational epitopes[1].

2.2 Interaction of hnRNP A3 with RNA

In order to investigate the interaction of this novel protein with RNA, the binding of the [^{32}P] - labelled oligoribonucleotide $_r$(UUAGGG)$_4$ to hnRNP A3 and its various deletion mutants was studied by employing UV crosslinking assay (Figure 1). This is a functionally

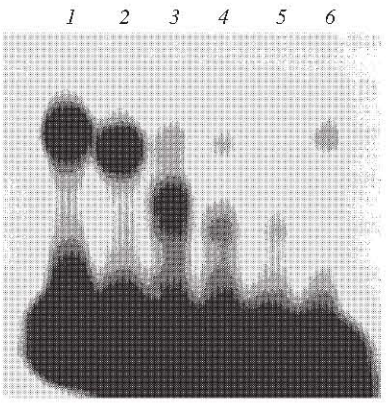

Fig. 1 Binding of [^{32}P]-labelled $_r$(UUAGGG)$_4$ to full length hnRNP A3 and its various deletion mutants

1: full length hnRNP A3; *2*: RBD1 and RBD2 (amino acides 1 ~ 209); *3*: RBD1 (amino acids 1 ~ 112); *4*: RBD2 (amino acids 112 ~ 209); *5*: C-terminal region (amino acids 209 ~ 296); *6*: RBD2 + C-terminus (amino acids 112 ~ 296).

significant telomeric repeat, which is found to be of particular significance of our previously studied 4 isoforms of other ribonucleoprotein - hnRNP D0 (our unpublished data). These RNA-protein interactions and their role in gene expression are being approached in terms of molecular biology. However, biophysical studies on them are rudimentary. The need for such physicochemical approach and the relevant thermodynamic reasoning on experimental designs were reviewed in detail recently[6]. Full length hnRNP A3, or its various deletion mutants, were incubated respectively with [^{32}P]-$_r$(UUAGGG)$_4$ for 30 min and subsequently UV-crosslinked. Samples were resolved on 10% SDS-polyacrylamide gels and analysed by autoradiography (Figure 2). As seen, all fragments tested bound [^{32}P]-$_r$(UUAGGG)$_4$. However, the strength of binding was highly variable. Thus, the [^{32}P]-riboprobe bound strongly to the full-length hnRNP A3 (lane *1*), as well as to the fragment containing RBD1 + RBD2 (lane *2*), while binding to either RBD1 or RBD2 was considerably weaker (lanes *3* and *4*). Interestingly, RBD1 bound much stronger to [^{32}P]-$_r$(UUAGGG)$_4$ than RBD2 alone. Interaction with the fragment containing the Gly-rich domain was hardly detectable (lane *5*) and interaction with the fragment comprising RBD2 and the Gly-rich domain was similar to that observed with RBD2 (lane *6*). Hence, this result suggests that RBD1 is the major region involved in RNA-binding, while RBD2 may have a stabilizing function.

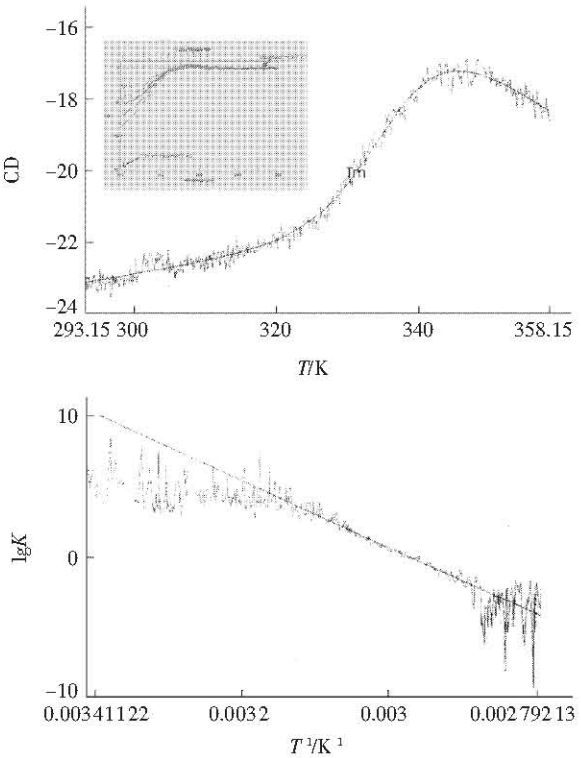

Fig. 2　Temperature denaturation curve of hnRNP A3

CD spectra were measured in a temperature range between 20 ~ 85℃, at 225 nm, at heating rate of 1℃/min. The range of hnRNP A3 was 300 ~ 220 nm, the speed of measurements was 50 nm/min. The concentration of hnRNP A3 was 2 g/L in 5 mmol/L phosphate buffer, 10 mmol/L NaCl. To quantify thermal stability of hnRNP A3, T_m was measured by monitoring the CD signal as a function of temperature, T_m refers to melting temperature. The inlet shows protein refolding of denatured hnRNP A3. Urea concentration was 0.5 g/L in 5 mmol/L phosphate buffer. Circular dichroism spectra were recorded at 25℃ within the range of 220 ~ 300 nm. The curve at the top represents fully denatured hnRNP A3, the curve at the bottom represents the fully refolded form.

2.3　CD and fluorescence measurements

Fluorescence spectrum of the RNP particle at the employed exitation wavelength of 280 nm is arround 340 nm, which is an indication that tryptophan is within a hydrophobic environment. This indicates that aromatic amino acids comprise the interior of the RNP particle. This, in turn was checked with dissociation experiment with 1 mol/L NaCl, to weaken the stabilizing bounds on the ribonucleoprotein particle. This fluorescence measurement at the wavelength of previously determined RNP particles' maximum of 340 nm as a function of NaCl concentration yielded no any change (data not shown for brevity). This observation leads to the conclusion that no any interactions of tryptophans with RNA, or with other proteins should be expected. However, this should be checked further in more elaborate studies employing solute fluorescence quenching. The main objective of CD assay is to investigate the secondary structure of hnRNP A3 and how it changes upon interactions with RNAs with possible importance in autoepitope recognition in terms of development of human systemic autoimmune pathology. For most proteins there is no significant CD spectrum between 250 nm and 300 nm compared to that observed with nucleic acids. Experiments involving the addition of protein can thus be conveniently carried out in this wavelength range. Below 250 nm, proteins and RNA have optical activity and any experiments here may require resolution of the spectrum into protein and RNA components.

Stability determination of hnRNP A3 was first undertaken by establishment of its urea and heat denaturation curves. Its full refolding was achieved by decreasing the urea concentrations via dialysis (Figure 1). The range of its heat denaturation was between 43.80 ~ 74.40℃ and its melting temperature was around 58℃ (Figure 3). The exact values of the unfolding free energy measured by temperature and urea denaturation were in agreement. The thermodynamic parameters determined in the present study were as follows: T_m (melting temperature of hnRNP A3) = (328.63 ± 0.2212) K; dH (enthalpy of denaturation of hnRNP A3) = (168 433 ± 12 166.4) J/mol; dS (entropy of hnRNP A3 heat denaturation) = (512.539 ± 37.0222) J/(mol · K) and ΔG of 40.91 kJ/mol (Figure 3). It is interesting to note that this high stability of hnRNP A3 is shared also by ribonucleases. The estimated thermodynamic values are similar to those obtained for hnRNP A3. Interesting finding was that upon interaction with RNA fragment $_r(UUAGGG)_4$ this apparent stability was further increased to higher temperature values (Figure 3), showing that RNA-binding have further implications in stabilizing the whole complex.

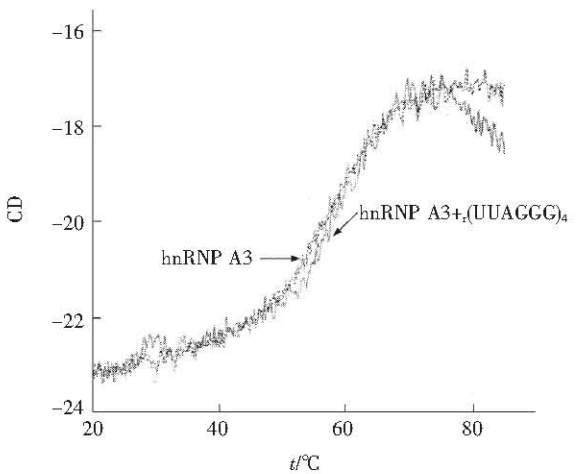

Fig. 3　Interaction of RNA $_r(UUAGGG)_4$ with hnRNP A3

The protein was employed at a concentration of 0.5 g/L in 5 mmol/L phosphate buffer. $_r(UUAGGG)_4$ was used at a concentration of 1 g/L. Temperature range of the experiment was 20 ~ 85℃. All other settings of the CD spectrometer were as described above. ——: A3 + RNA Tup; - - -: A3 Tup.

2.4 Epitope mapping

Figure 4 depicts epitope mapping results of hnRNP A3. The results indicate that there are at least two major epitopes——(RBD1 + RBD2) and (RBD2 + gly-rich domain), respectively. Comparison with autoepitopes identified in hnRNP A1 and hnRNP A2 revealed interesting differences (Figure 4).

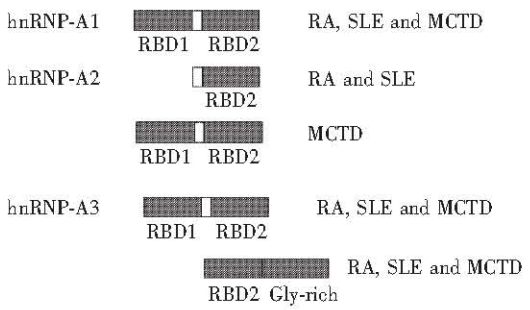

Fig. 4 Major autoepitopes identified in human hnRNP A/B proteins

3 Discussion

Extensive experimental data exist concerning functional characterization of particular members of the hnRNP A/B family with respect to their RNA-binding properties, as well as their association with pre-mRNA splicing complexes and their role as autoantigens in various autoimmune disorders. The attention of the scientific community is attracted to search for the specific involvement of hnRNP particles in different genetic diseases, as well as in cancer. The exponentially growing information concerning structure and function of various hnRNPs will be a valuable insight into the pathological mechanisms via which these proteins play role as targets of autoantibodies. In this context, of particular importance is determination of the physicochemical features of RNA-protein folding patterns[6], subsequently relating them to development of disease-specific epitope formation.

As outlined before, the general structure of all hnRNP A/B proteins is devided into two domains: the first 195 residues comprise the so-called UP1 domain, consisting of two canonical RNA-recognition motives-(RRM 1 and RRM 2), each of which contains the conserved RNP-2 and RNP-1 submotives. The Gly-rich C-terminal domain comprises an RGG box and nuclear localization motif. The entire Gly-rich motif contributes to protein-protein interaction patterns. Two conserved and solvent exposed Phe residues, found at the centre of the β-sheet in each RRM have been shown to contact RNA directly[7,8]. The least conserved 3rd loop in U1A is engaged in extensive RNA interactions and changes its conformation upon RNA binding. The RNP domain interacts with a flexible single-stranded RNA and the β-sheet provides a large surface for extensive interaction with nucleotides. Regions outside of the RRM may also play important roles in RNA binding.

In this context, it was interesting to analyse the immunological crossreactivities between all these various proteins, especially the human proteins with their ability to function as autoantigens in certain systemic autoimmune disorders. Regarding this part of the work presented here, it was worth analysing the role of individual domains of hnRNP A/B proteins with respect to antibody recognition. Despite the close sequence similarities between hnRNP A3 and hnRNP A1 or hnRNP A2, only very few patients' sera were found to react with all these three proteins.

Detailed epitope mapping studies of hnRNP A3 provide evidence that there are at least two major epitopes, which are contained in (RBD1 + RBD2) and (RBD2 + Gly-richdomain), respectively. Comparison with autoepitopes identified in hnRNP A1 and hnRNP A2 revealed interesting differences (Figure 4). Thus in hnRNP A2, the RBD2 was found to contain the major epitope recognized by patients with rheumatoid arthritis or systemic lupus erythemathosus. This particular region was also found to be essential for interaction with RNA and patients' autoantibodies strongly inhibited RNA binding. Autoantibodies from patients with mixed connective tissue disease, on the other hand, recognized an epitope comprising RBD1 and RBD2. Interestingly, the major epitope of hnRNP A1 also comprises both RBDs, which are, however, targeted also by patients with rheumatoid arthritis and systemic lupus erythemathosus (Skriner K. Personal communication). Taken together, these data confirm that RA, SLE and MCTD are immunologically linked by autoimmunity to the functionally important RNA binding regions of hnRNP A/B proteins. Interestingly, autoantibodies against hnRNP A3 were found to occur less frequently than autoantibodies to hnRNP A1 or hnRNP A2. Thus, only 10% of RA, SLE, MCTD and scleroderma patients recognized hnRNP A3. The reason for this is unknown at present and may be due to the fact that the recombinant protein employed may be different from the natural protein expressed in human tissues. Why are closely related and evolutionarily conserved RBD domains differentially recognized by the autoantibodies? This interesting question has not been approached so far. The phenomena can be discussed having considered the physicochemical characteristics and overall folding patterns of these domains in terms of protein antigenicity. Sequence comparisons between U1A, hnRNP C, hnRNP A1 and *Drsosophila*-sex lethal (sxl) protein structures have revealed that they all have the same fold, but subtly different placing of the β2 and β4 strands, the most eminent characteristic being

the variability of the 3rd loop length. Individual RRMs have preferences for different RNA sequences, due to differences in surface amino acid residues found outside of the conserved RNP submotifs, although still on the β-sheet, in loop 3 and in certain cases also in loop 1[8]. This may also explain the differential recognition of RRMs by autoantibodies. In certain cases, the two RRMs somehow seem to act in concerted fashion to give rise to the overall RNA- and antibody-binding characteristics, whereas in other cases the presence of only one RRM is sufficient for autoantibody and RNA recognition. Thus, RBD1 alone bound strongly to RNA, however joining of RBD2 to RBD1 increased the overall affinity, indicating that also RBD2 contributes substantially to RNA-binding.

Figure 1 ~ 3 depicts the stability, physicochemical properties and RNA-binding features of hnRNP A3 protein. CD and fluorescence spectroscopic measurements demonstrated that hnRNP A3 protein is a rather stable protein. The free energy of unfolding of the full-length hnRNP A3 was characterized by both urea and temperature denaturation. Both methods showed that this protein was stable with T_m of 58℃. The precise values of the unfolding free energy measured by these two methods were in good agreement.

Interesting finding was that upon interaction with RNA fragment $_r(UUAGGG)_4$ this apparent stability was further increased to higher temperature values (Figure 2), suggesting a stabilizing role of the RNA-protein interactions for hnRNP particles. The results are in agreement also with other relevant works concerning this oligoribonucleotide fragment[9,10]. At present, crystal structural data is missing for $_r(UUAGGG)_4$. However, recent structural data[11] indicate a substantial thermodynamic stability of a spatially related UUCG tetraloop. The observed structure is close to that obtained by NMR in solution, showing also the stabilizing role of the 2′-hydroxyl groups in the tetraloop. Although a similar spatial reasoning may be applied for $_r(UUAGGG)_4$, further detailed crystallographic and NMR data are needed for elucidation of the interaction of hnRNP A3 with this oligoribonucleotide fragment and its functional significance. It is well-known that most large RNAs achieve their active, native structures only as complexes with one or more cofactor proteins[12,13]. This implies that an initial phase of core RNP assembly is mediated by a high affinity of ribonucleoproteins for the single-stranded uridine tract, and is essential for the thermodynamic stability and overall folding pattern of the RNP particle. More experiments are being carried out on full length hnRNP A3 and its various deletion mutants with respect of their involvement in splicing and nucleocytoplasmic transport processes. Thus, we currently study the alternative splicing activities of this ribonucleoprotein particle by analysing whether the individual RRMs of hnRNP A3 have similar properties of promoting distal 5′ splice-site selection via antagonizing the activity of SF2/ASF, as already determined for hnRNP A1 and A2. Elucidation of the role of hnRNP A3 as autoantigen, particularly with respect to its expression in inflamed tissue, may provide further clues for understanding the role of hnRNP A/B proteins in the pathogenesis of systemic autoimmune diseases.

Aknowledgments Aknowledgments are due to Professor G. Steiner and Dr. K. Skriner for their help during cloning and molecular characterization of human hnRNP A3 at Vienna Biocenter, and to Dr. M. Takahashi for his warm hospitality, generous financial suport and close supervision during biophysical measurements in Orsay. I am grateful to Ö. A. Austauschdienst-Geschäftsstelle Wien for awarding me with Austrian Governmental Ph. D. Scholarship and for providing me with excellent living conditions in Vienna.

References

1 Süleymanoğlu E. Cloning and Characterization of Human Heterogeneous Nuclear Ribonucleoprotein (hnRNP) A3-a Novel Member of the hnRNP A/B family: [Ph. D. Thesis]. Vienna: University of Vienna, 2001

2 Biamonti G, Ghigna C, Caporali R, *et al*. Heterogeneous nuclear ribonucleoprotein (hnRNPs): an emerging family of autoantigens in rheumatic diseases. Clin Exp Rheum, 1998, **16** (3): 317 ~326

3 Krecic A M, Swanson M S. hnRNP complexes: composition, structure and function. Curr Opin Cell Biol, 1999, **11** (3): 363 ~371

4 van Venrooij W. Autoantigens in connective tissue diseases. In: Panayi G S, ed. Immunology of The Connective Tissue Diseases: Dordrecht. Kluwer Academic Publ, 1994, 305 ~334

5 Süleymanoğlu E. The Inaugural Austral-Asian Biospectroscopy Conference (ABC) -Suranaree University of Technology, Nakhon Ratchasima (Korat), 3rd-7th Feb, Thailand, 2003

6 Stolarski R. Thermodynamics of specific protein-RNA interactions. Acta Biochim Polonica, 2003, **50** (2): 297 ~318

7 Mayeda A, Munroe S H, Xu R-M, *et al*. Distinct functions of the closely related tandem RNA-recognition motifs of hnRNP A1. RNA, 1998, **4** (9): 1111 ~1123

8 Varani G, Nagai K. RNA recognition by RNP proteins during RNA processing. Ann Rev Biophys Biomol Struct, 1998, **27**: 407 ~445

9 Ishikawa T, Matunis M J, Dreyfus G, *et al*. Nuclear proteins that bind the pre-mRNA 3′ splice site sequence $_r(UUAG/G)$ and the human telomeric DNA sequence $_d(TTAGGG)_n$. Mol Cell Biol, 1993, **13** (7): 4301 ~4310

10 Nagata T, Kurihara Y, Matsuda G, *et al*. Structure and interactions with RNA of the N-terminal UUAG-specific RNA-binding domain of hnRNP D0. J Mol Biol, 1999, **287** (2): 221 ~237

11 Ennifar E, Nikulin A, Tishchenko S, *et al*. The crystal structure of UUCG tetraloop. J Mol Biol, 2000, **304** (1): 35 ~42

12 Webb A E, Weeks K M. A collapsed state functions to self-chaperone RNA folding into a native ribonucleoprotein complex. Nature Struct Biol, 2001, **8** (2): 135 ~140

13 Ro-Choi T S. Nuclear snRNA and nuclear function (discovery of 5′ cap structures in RNA). Crit Rev Euk Gene Exp, 1999, **2**: 107 ~158